Available online at SciVerse ScienceDirect

SciVerse ScienceDirect

J. Mater. Sci. Technol., 2013, 29(8), 737−741

JMST

www.JMST.org

Observation of an EPIR Effect in $Nd_{1-x}Sr_xMnO_3$ Ceramics with Secondary Phases

S.S. Chen[1,2], *X.J. Luo*[2], *D.W. Shi*[2], *H. Li*[1], *C.P. Yang*[2)*]

1) School of Mathematics and Physics, Hubei Polytechnic University, Huangshi 435003, China

2) Faculty of Physics and Electronic Technology, Hubei University, Wuhan 430062, China

[Manuscript received December 19, 2011, in revised form April 10, 2012, Available online 17 April 2013]

$Nd_{1-x}Sr_xMnO_3$ ($x = 0.3$, 0.5) ceramics containing a secondary phase are synthesized by high-energy ball milling and post heat-treatment method. The 4-wire and 2-wire measuring modes are used to investigate the transport character of the grain/phase boundary (inner interface) and electrode-bulk interface (outer interface), respectively, and the results indicate that there is a similar nonlinear $I-V$ behaviour for both of the inner and outer interfaces, however, the electric pulse induced resistance change (EPIR) effect can only be observed at the outer interface.

KEY WORDS: Electric pulse induced resistance change (EPIR); Space charge layer; Nonlinearity; Manganite; High-energy ball milling

1. Introduction

Perovskite-type manganites have been widely studied for many years, and meanwhile the core physical theories including the orbital ordering, Jahn−Teller (JT) effect, the intrinsic phase separation and double exchange (DE) interaction have been established. But until the 1990s, they become hot topics of condensed matter due to the rediscovery of a colossal magnetoresistance (CMR), which exhibits higher magnetoresistance (MR) effect and wider application prospect than that of the giant magnetoresistance (GMR) and tunneling magnetoresistance (TMR)[1,2]. However, the CMR did not hold its promise as a sensor so far. It was found that: (1) the sensitivity to a magnetic field is still low: it generally requires several Teslas outer magnetic field to get a large resistance change; (2) the temperature range of the large CMR is very narrow, and (3) the CMR is often partly irreversible. Therefore, nowadays the colossal electroresistance (CER) is intensely investigated as the electric field is much easy to control than the magnetic field[3−8]. Especially, the electric pulse induced resistance change (EPIR) effect, which is related to the CER, attracts extensive attention since Liu and his co-workers found this unique phenomena in $Pr_{0.7}Ca_{0.3}MnO_3$ (PCMO) thin films[9]. Since then, a large number of experiments such as changing the oxide type, carrier type, electrode type were carried out to investigate the origin of EPIR but it is still controversial. Presently, many models for EPIR are proposed to explain the existing experiments[10−13]: conductive domain tunneling effect[14], intrinsic body effect[9,15], interface effect[10] and redox effect[16], but none of them can satisfactorily explain all aspects of the EPIR behavior.

Specifically, the electrode-bulk interface (here, named as outer interface) influence on EPIR has been examined in detail by many groups[10−13,17], but the effect of grain/phase boundary (here, named as inner interface) on EPIR behaviour is rarely studied. In this work, the transport character of the inner interfaces of $Nd_{1-x}Sr_xMnO_3$ ($x = 0.3$, 0.5) ceramics with secondary phases is investigated. The results show that although the space charge layers exist in both inner and outer interfaces and thus exhibit nonlinear $I-V$ behaviour, only the outer interface shows the EPIR effect.

2. Experimental

Usually, the perovskite-type manganites are synthesized by the solid state reaction[18], sol−gel method[19], chemical synthesis[20], and high-energy ball milling[21,22]. The ball milling method can produce compounds with large numbers of physical and chemical defects, enhancing the defect density at the inner interfaces. Thus, the presented samples $Nd_{1-x}Sr_xMnO_3$ ($x = 0.3$, 0.5) are synthesized by high-energy ball milling and post heat-treatment at 1623 K for 7 h. The detailed preparation process can be found in our previous work[23]. Four bar-shape electrodes with silver glue are fabricated on the same surface of samples. The dimension of each electrode is about 3, 1.6 and 0.5 mm in length, width and thickness, respectively, and about 1.2 mm

* Corresponding author. Tel.: +86 027 88665447; E-mail address: cpyang@hubu.edu.cn (C.P. Yang).

http://dx.doi.org/10.1016/j.jmst.2013.04.010

spacing is left for each two electrodes. For the coated silver glue electrode, the contact resistance is ineluctable; for the silver electrode, however, it usually exhibits ohmic behavior[24]. The microstructure and phase purity of samples are examined by scanning electron microscopy (SEM, JSM-5610LV, Japan), energy dispersive spectroscopy (EDS) and X-ray diffraction (DRON-3 type, Cr$K\alpha$). The magnetic character of samples is measured by using a Vibrating Sample Magnetometer (VSM). The DC measurement (containing $R-T$, $I-V$ and EPIR) are performed by using a Keithley 2400 multimeter, and the pulse width of 150 μS, pulse amplitude of 3 V and bias voltage of 0.1 V are selected, respectively.

3. Results and Discussion

The $Nd_{1-x}Sr_xMnO_3$ (NSMO) compounds belong to the medium-bandwidth systems. At low temperatures, the NSMO compound transforms from a ferromagnetic metal to a CE-type antiferromagnetic charge-orbital ordered insulator and then to a charge ordering type (CO-type) insulator with increasing Sr doping from 0.3 to 0.6; however, at higher temperatures, NSMO exhibits O′ or O*-type paramagnetic insulating phases, as shown in Fig. 1. Based on the $Nd_{1-x}Sr_xMnO_3$ electronic phase diagram[25], the optimal doping, $Nd_{0.7}Sr_{0.3}MnO_3$, and the semi-doping, $Nd_{0.5}Sr_{0.5}MnO_3$, compositions are selected.

The SEM images, the EDS spectrum and the compositional analysis of the $Nd_{0.7}Sr_{0.3}MnO_3$ ceramics are shown in Fig. 2. As an example, only SEM results of sample with $x = 0.3$ are given. From Fig. 2 some secondary phases can be easily observed in addition to the $Nd_{0.7}Sr_{0.3}MnO_3$ matrix grains. These bar-shape secondary phases grow out of the matrix grain boundaries and extend in different directions. In order to confirm the difference between the secondary phase and matrix grains, EDS analysis was carried out and the results show that the composition of the matrix grains is well close to the stoichiometric sample (Fig. 2(a)). However, for the secondary phase, it is very different from that of the matrix grain and in particular no manganese can be found (Fig. 2(b)). The secondary phases can also be reflected in XRD as shown in Fig. 3. For the $Nd_{0.7}Sr_{0.3}MnO_3$ samples prepared by solid state reaction no impurity phases can be detected, while for the $Nd_{0.7}Sr_{0.3}MnO_3$ from ball milling synthesis, in addition to the diffraction peaks from matrix grains, some unknown diffraction peaks appear, which proves that a secondary phase exists in the ball-milled compound. On the composition of the secondary phase, we cannot confirm which compound it is till now as its element proportion does not well coincide with existing compounds.

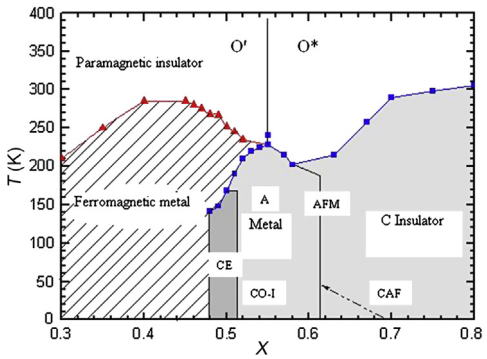

Fig. 1 $Nd_{1-x}Sr_xMnO_3$ electronic phase diagram (CO-charge ordering, AFM − antiferromagnetism, CO−I-charge ordering insulator, CAF-canted antiferromagnetism).

It may be considered reasonably that the new-grown secondary phases make the grain boundary more disordered, and lead to a significant effect on electromagnetic transport behavior[26,27]. Fig. 4 shows the resistance and magnetization dependence of temperatures for the $Nd_{0.7}Sr_{0.3}MnO_3$ and $Nd_{0.5}Sr_{0.5}MnO_3$ samples, respectively. With $x = 0.3$, the resistance reaches 10^6 Ω below low temperature of 70 K, which is much larger than that of the stoichiometric sample, and also the insulator-metal (T_{MI}) transition cannot be observed during the whole measuring temperatures even though a T_C of about 110 K can be detected from the $M-T$ curve (see the inset of Fig. 4(a)). The Currie temperature T_C of 110 K is much lower than that of 230 K for stoichiometric sample[28]. This may ascribe to the formation of insulating grain/phase boundaries due to the ball milling process. For the sample with $x = 0.5$, similar to the sample of $x = 0.3$, it becomes more insulating with decreasing the temperature and also without a T_{MI} transition (Fig. 4(b)). On the other hand, magnetic character exhibits a more complicated and diffuse behaviour, together with a smaller magnetization.

Generally, the $I-V$ measurement could characterize the electrical transport properties of a material. For uniform materials, the resistance comes from lattice vibrations (phonons) and the scattering of impurity ions, so the $I-V$ behaviour follows the Ohm's law; however, for non-uniform materials, space charge layers usually exist, resulting in built-in electric fields at the interfaces, and the $I-V$ curve does not meet Ohm's law. Also, in mixed manganites the space charge regions are very sensitive to external electric/magnetic fields, thereby, leading to the so-called interface-dependent CMR and CER effects. Fig. 5 shows the $I-V$ and EPIR properties of $Nd_{0.7}Sr_{0.3}MnO_3$ sample under the 4-wire and 2-wire measuring modes, respectively. The voltage scanning step of 0.02 V/s is adopted. Usually the 4-wire measuring method can result in the elimination of the contact resistance from electrode-bulk interface and main reflection of the bulk transport, while the resistance from 2-wire measurement mainly contains that from the bulk and the outer interface. In this case, the 4-wire resistance mainly comes from the inner interface and the 2-wire one is from the outer interface due to the too small bulk contribution of 58.5 Ω (see Fig. 5(b)). From Fig. 5, it can be seen that the $I-V$ curve is nonlinear and with a hysteretic character for both the inner and outer interfaces (see Fig. 5(a) and (c)), indicating that a large barrier and built-in electric field exist. The nonlinearity and hysteresis of $I-V$ behavior are often found in manganites[29−33]. Generally, it appears in two ways: one is the outer interface, in which because of the differences of Fermi surface and work function, the carrier concentration between the electrode and bulk may produce a Schottky barrier and lead to the separation of positive and negative charges; the other is at the inner interface, and the preferential segregation of defects and impurity ions at the interface can introduce different electronic states between different phases, thus, forming space charge layer, which is similar to the back to back Schottky barrier model[34].

Although both of the inner and outer interfaces show similar nonlinear $I-V$ behaviour, there are great differences in the EPIR effect, as shown in Fig. 5(b) and (d). For the outer interface a stable EPIR effect is observed, and at room temperature the R_{high} and R_{low} are 730 and 585 Ω, respectively, so the EPIR value is 25% (EPIR = $(R_{high} - R_{low})/R_{low} \times 100\%$). For the inner interfaces, however, the resistance has nothing to do with the polarity of applying pulses and almost keeps a constant value of 58.5 Ω even if the same pulse parameters as that of the outer